Slow earthquakes illuminating interplate coupling heterogeneities in subduction zones

Satoru Baba[1,1], Shunsuke Takemura[1,1], Kazushige Obara[2,2], and Akemi Noda[3,3]

[1]Earthquake Research Institute, the University of Tokyo
[2]Earthquake Research Institute, The University of Tokyo
[3]National Research Institute for Earth Science and Disaster Resilience

November 30, 2022

Abstract

Slow earthquakes are mainly distributed in the vicinity of seismogenic zones of megathrust earthquakes and relationships between both types of earthquakes are expected. We examined the activity of very low frequency earthquakes (VLFEs), classified as one type of slow earthquake, around Japan because they have the potential to clarify detailed spatiotemporal slip behaviors at the plate boundaries. The distribution of the shallow VLFE activity rate is heterogeneous along trench axes and exhibits an anticorrelation relationship with the spatial distribution of the interplate coupling ratio, whereas deep VLFEs are distributed only in weakly coupled areas and the spatial variation of the activity rate is small. Furthermore, VLFEs are mainly hosted by low seismic velocity anomalies. Thus, slow earthquakes can be triggered by decreased effective stress due to the high pore fluid pressure within regions with weak interplate coupling and their activity can be an indicator of interplate slip behavior.

Slow earthquakes illuminating interplate coupling heterogeneities in subduction zones

Satoru Baba[1], Shunsuke Takemura[1], Kazushige Obara[1], and Akemi Noda[2]

[1]Earthquake Research Institute, The University of Tokyo, 1-1-1, Yayoi, Bunkyo-ku, Tokyo, 113-0032, Japan

[2]Earthquake and Tsunami Research Division, National Research Institute for Earth Science and Disaster Resilience, 3-1 Tennodai Tsukuba, Ibaraki 305-0006, Japan

Corresponding author: Satoru Baba (babasatoru@eri.u-tokyo.ac.jp)

Key Points:

- Comprehensive detection of very low frequency earthquakes (VLFEs) around Japan clarifies detailed spatiotemporal slip behaviors
- VLFE distribution reflects strong and weak spatial heterogeneity of frictional property along shallow and deep plate boundary, respectively
- Shallow VLFEs can be caused by decreasing effective stress due to high pore fluid pressure around weak interplate coupling

Abstract

Slow earthquakes are mainly distributed in the vicinity of seismogenic zones of megathrust earthquakes and relationships between both types of earthquakes are expected. We examined the activity of very low frequency earthquakes (VLFEs), classified as one type of slow earthquakes, around Japan because they have the potential to clarify detailed spatiotemporal slip behaviors at the plate boundaries. The distribution of the shallow VLFE activity rate is heterogeneous along trench axes and exhibits an anticorrelation relationship with the spatial distribution of the interplate coupling rate, whereas deep VLFEs are distributed only in weakly coupled areas and the spatial variation of the activity rate is small. Furthermore, VLFEs are mainly hosted by low seismic velocity anomalies. Thus, slow earthquakes can be triggered by a decreased effective stress due to the high pore fluid pressure within regions with weak interplate coupling and their activity can be an indicator of interplate slip behavior.

Plain language summary

Along subducting plate boundaries, slow earthquakes are mainly distributed in the vicinity of large slip areas of huge earthquakes. Characteristics of slow earthquakes suggest that their frictional conditions at plate boundaries differ from those of regular earthquakes. We detected very low frequency earthquakes (VLFEs), classified as one type of slow earthquakes, around Japan because their activity can be related to interplate coupling. The VLFEs along the Nankai Trough are distributed in the offshore areas in the depth ranges of 5–10 km (shallow VLFEs) and in the inland areas in the depth ranges of 30–40 km (deep VLFEs), whereas VLFEs off Tohoku are distributed only in the offshore (shallow) areas. The distribution of the shallow VLFE activity is more complicated along trench axes than deep VLFE activity. This suggests that the along-strike heterogeneity of the frictional properties is stronger in the shallow part than in the deep part of the plate boundary. Furthermore, the shallow VLFE activity shows an anticorrelation relationship with the spatial distribution of the interplate coupling rate. Shallow VLFEs occur mainly in the area where seismic velocity is low, therefore shallow slow earthquakes can be triggered by the high pore fluid pressure within weak interplate coupling zones.

1 Introduction

Slow earthquakes mainly occur between seismogenic and stable sliding zones along the plate boundaries of subduction zones (Obara & Kato, 2016) and are considered to be transitional phenomena between them. The spatial variation of the slip properties at the plate boundary must be controlled by heterogeneous frictional conditions (Obara & Kato, 2016). Various slow earthquakes, such as low frequency tremors (2–8 Hz), very low frequency earthquakes (VLFEs; 0.02–0.05 Hz), slow slip events (SSEs), and coupled phenomena (episodic tremor and slip; ETS) have been detected in many subduction zones worldwide (e.g., Ito et al., 2007; Obara, 2002; Obara & Ito, 2005; Rogers & Dragert, 2003; Wallace et al., 2012). Previous studies confirmed that the hypocenters and focal mechanisms of slow earthquakes are consistent with shear slips along the plate boundaries. However, the relationship between slow earthquakes and the neighboring seismogenic zone has not yet been fully understood.

The Philippine Sea Plate and Pacific Plate are subducting beneath the island arc around Japan (Figure 1). The characteristics of the subducting plates completely differ. The Philippine Sea Plate subducting in the Nankai Trough is young and warm, whereas the Pacific Plate subducting in the Japan and Kuril trenches is old and cold (Syracuse et al., 2010). The plate convergence rates of these plates also differ, 4–5 cm/year and 8–9 cm/year in the Nankai Trough and in the Japan and Kuril Trenches, respectively (DeMets et al., 1994). Despite these differences, both subduction zones have repeatedly experienced huge earthquakes. Recent huge earthquakes are 1944 Tonankai (moment magnitude, Mw, of 8.0; Kikuchi et al., 2003) and 1946 Nankai earthquakes (Mw 8.4; Tanioka & Satake, 2001) along the Nankai Trough, and 2003 Tokachi-Oki (Mw 8.0; Yagi, 2004) and 2011 Tohoku earthquakes (Mw 9.0; Iinuma et al., 2012) along the Kuril and Japan trenches. Slow earthquakes have also been observed in the regions surrounding huge earthquakes in both subduction zones (Obara & Kato, 2016).

Along the Nankai Trough, slow earthquakes occur in both the shallower and deeper extensions of the seismogenic zone. The characteristics of deep slow earthquakes have been extensively investigated using nationwide onshore seismic and geodetic networks (Ito et al., 2007; Obara, 2002; Obara & Ito, 2005). Shallow slow earthquakes along the Nankai Trough have been investigated using both onshore and offshore seismic records (Asano et al., 2008; Nakano et al., 2018; Obara & Ito, 2005; Sugioka et al., 2012; Takemura et al., 2019a). The results of recent studies revealed that simultaneous occurrence of shallow tremors, VLFEs and SSEs was observed as similar to deep ETS (Araki et al., 2017; Nakano et al., 2018), and that shallow slow earthquakes are activated by high pore fluid pressure in regions surrounding strongly locked zones (Takemura et al., 2019a).

Along the Japan and Kuril trenches, shallow VLFEs temporarily changed after the 2003 Tokachi-Oki and 2011 Tohoku earthquakes, respectively (Asano et al., 2008; Matsuzawa et al., 2015). In recent studies based on onshore and offshore data, more shallow tremors and VLFEs were detected (Baba et al., 2020; Nishikawa et al., 2019; Tanaka et al., 2019). Results suggested that the slow earthquake activity and large coseismic slip area of a huge earthquake are separated in the along-strike direction. Although the relationships between both types of earthquakes have been extensively investigated in both subduction zones, differences in the spatiotemporal variation of the slow earthquake activity between both subduction zones have not been discussed in detail. This difference may be related to the activity of huge earthquakes or the stress state of the plate boundaries.

Slow earthquakes are inhomogeneously distributed at the plate boundary (Obara & Kato, 2016). Therefore, the spatial variation of their activity can reflect the heterogeneity of the frictional conditions on the megathrust fault plane. Investigations of the activity of slow earthquakes within the subduction zones can provide new insights into the stress accumulation or frictional conditions at the plate boundary. To compare VLFE activities across Japan, we comprehensively detected VLFEs in Southwest Japan in this study using the same method as in our previous studies (Baba et al., 2018; Baba et al., 2020), which elucidated the distribution of deep VLFEs in Southwest Japan and shallow VLFEs along the Japan and Kuril trenches. The VLFEs were detected using decade-scale onshore seismic records. These records were used because shallow VLFEs can be detected due to the effective propagation of surface waves, the observation period of onshore networks is longer than that of offshore networks, and the comparison of deep and shallow VLFEs is possible using the same dataset. Based on the newly constructed catalogue, we discussed the characteristics of regions with slow earthquake activity from geodetic and geophysical viewpoints. The shear stress is accumulated at the plate boundary as a result of interplate locking. In addition, the presence of pore fluid, which decreases the seismic velocity, can change the frictional conditions of the plate boundary. Therefore, the comparisons of the VLFE activity with the slip-deficit rate and seismic velocity structure provide insights into the mechanical properties at the plate boundary.

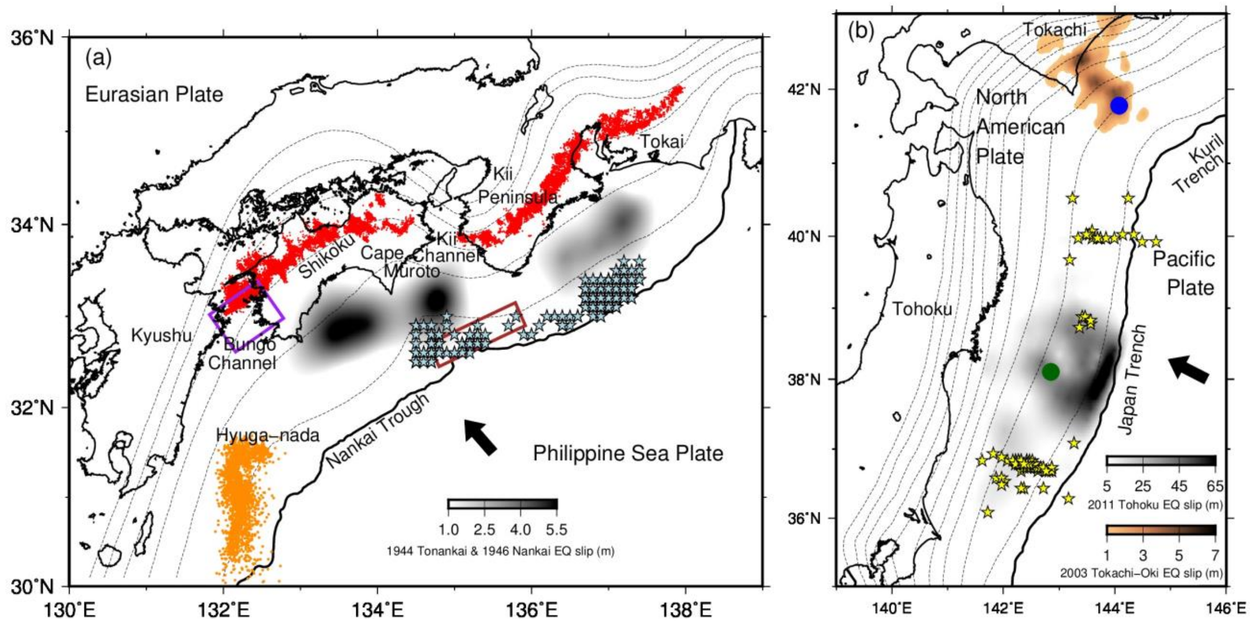

Figure 1. Huge and slow earthquake activities based on previous studies. (a) Huge and slow earthquakes along the Nankai Trough. Red and orange dots represent the epicenters of the tremors in Southwest Japan (Obara et al., 2010) and Hyuga-nada (Yamashita et al., 2015). Light blue stars represent the epicenters of the VLFEs (Takemura et al., 2019a). Grey shadings indicate the coseismic slip distributions of the 1944 Tonankai earthquake (Kikuchi et al., 2003) and the 1946 Nankai (Tanioka & Satake, 2001) earthquakes. The solid black curve represents the Nankai Trough. Dashed contours indicate the isodepths of the top of the Philippine Sea Plate with a 10 km intervals (Koketsu et al., 2012). The black arrow indicates the convergence direction of the Philippine Sea Plate, which subducts below the Eurasian Plate in the Nankai Trough. Purple and brown rectangles represent the estimated fault plane of the SSEs in the Bungo channel (Hirose et al., 2010) and off the Kii channel (Yokota & Ishikawa, 2020), respectively. (b)Huge and slow earthquakes along the Japan and Kuril trenches. Yellow stars represent the epicenters of the VLFEs (Matsuzawa et al., 2015). Blue and green circles indicate the epicenters of the 2003 Tokachi-Oki and 2011 Tohoku earthquakes, respectively. Brown and grey shadings indicate the coseismic slip distributions of the 2003 Tokachi-Oki (Yagi, 2004) and Tohoku (Iinuma et al., 2012) earthquakes, respectively. The solid black curve represents the Japan and Kuril trenches. Dashed contours indicate the isodepths of the top of the Pacific Plate in a 10 km intervals (Koketsu et al., 2012). The black arrow indicates the convergence direction of the Pacific Plate, which subducts underneath the North American Plate in the Nankai Trough.

2 Data and Methods

2.1. Data

We used continuous seismograms of F-net broadband seismometers (Okada, 2004) from January 2003 to June 2019 after removing instrumental responses and resampled at one sample per second. A bandpass filter with a frequency range of 0.02–0.05 Hz was applied to all seismograms to enhance VLFE signals of onshore seismic stations.

2.2. Detection of VLFEs

Generally, the detection procedure used for VLFEs was the same as that reported in our previous study (Baba et al., 2020). We placed 196 virtual epicentral grids on the Philippine Sea Plate boundary in Southwest Japan (Figure S1) in intervals of 0.3° and computed synthetic waveforms for the ten stations closest to each virtual source grid using the open-source finite difference method code (OpenSWPC; Maeda et al., 2017) and by using a three-dimensional velocity structure model of the Japan Integrated Velocity Structure Model (JIVSM; Koketsu et al., 2012). We computed waveforms on a 3-D grid with spacing of 0.2 by 0.2 km. We used the Küpper wavelet with a duration of 10 s and Mw of 4.0 as source time function. The focal mechanisms were assumed to be consistent with the geometry of the plate boundary of the JIVSM and plate motion model, NUVEL-1A (DeMets et al., 1994). We then calculated cross-correlation coefficients between the filtered synthetic template waveforms and F-net seismograms every 1 s. We selected events with station- and component-averaged coefficients exceeding the threshold defined as nine times of the median absolute deviation of the distributions.

False detections by regional regular and teleseismic earthquakes were removed using the catalogue of the Japan Meteorological Agency and the United States Geological Survey, respectively. However, considerable false detections remained, even after removing the teleseismic events based on the catalogues. Although the event amplitudes and cross-correlation coefficients generally are positively correlated (Baba et al., 2020), events with high amplitudes and average cross-correlation coefficients occur, which are considered to be false detections that are mainly caused by teleseismic events. Therefore, we did not count events with average cross-correlation coefficients below 0.4 and relative amplitudes to templates higher than 0.2 or average cross-correlation coefficients below 0.38 and relative amplitudes to templates higher than 0.1, except for Hyuga-nada. In the Hyuga-nada region (south of 32°N in the study area), the events had average cross-correlation coefficients below 0.4 and relative amplitudes to templates higher than 0.8. We established different thresholds for Hyuga-nada because typical VLFE amplitudes are larger than those in other areas.

2.3. Estimation of the moments of events

We calculated the relative amplitude of an event with respect to synthetic waveforms with source durations of 10 s and Mw 4.0 (c):

$$c = \frac{\sum_{ij} \int g_{ij}(t) f_{ij}(t) dt}{\sum_{ij} \int g_{ij}(t)^2 dt} \quad (1)$$

where $f_i(t)$ and $g_i(t)$ are the observed waveform and synthetic template waveform at the i-th station and j-th component, respectively. The relative amplitude c was calculated to minimize the variance reduction between the synthetic template waveform and observed waveform. The moment of each event (M_o^{event}) was estimated from the amplitude of the event relative to the template:

$$M_O^{event} = c M_O^{syn} \quad (2)$$

where M_o^{syn} is the moment of the synthetic waveforms of Mw 4.0. Subsequently, we estimated the VLFE magnitude (M^{event}) using the following relationship between magnitude and moment (Hanks & Kanamori, 1979):

$$M^{event} = \frac{log_{10} M_O^{event} - 9.1}{1.5} \quad (3)$$

The frequency distribution of VLFEs is shown in Figure S2. When we estimated the magnitudes of VLFEs, we excluded the virtual epicentral grids with a number of detected events below 35 or in which most of the events were falsely detected, mainly due to the teleseismic events that remained after discarding false detections using the process described above. The ratio of false detections was examined by visually investigating the detected event waveforms. Although many events were detected near the coast of Kyushu, most of them were false detections. The tendencies of the estimated moment density release rates off Cape Muroto, off the southern Kii Peninsula, and off the southeastern Kii Peninsula are similar to those reported in a previous study (Takemura et al., 2019a).

Regarding the VLFEs along the Japan and Kuril trenches, we evaluated the magnitudes of VLFEs detected in our previous study (Baba et al., 2020) based on the equations (1) – (3). The cumulative moment of each grid was calculated using the sum of moments of each VLFE.

2.4. Error estimation

We evaluated the errors of the cumulative moment of each grid by using the nonparametric bootstrap method (Tichelaar & Ruff, 1989). First, 500 bootstrap samples were prepared for each grid. A bootstrap sample was generated from the original events. If *n* events were detected in a grid, a bootstrap sample consisted of *n* events including duplicates. Subsequently, cumulative moments were calculated from by the sum of the moments of n events. Finally, we estimated the standard deviations of the 500 cumulative moments.

We also estimated the errors of the cross-correlation coefficients between the moment density release rate and the coupling rate using the nonparametric bootstrap method. The 500 bootstrap samples, which were generated from the 49 original grids, were prepared and a bootstrap sample consisted of 49 grids including duplicates. Cross-correlation coefficients were calculated for each bootstrap sample. We then estimated the standard deviations of the 500 cross-correlation coefficients.

3 Results

The VLFEs along the Nankai Trough are distributed in the depth ranges of 30–40 km (deep VLFEs) and 5–10 km (shallow VLFEs; Figure S3). We classified deep VLFE activity into four regions (i.e. western Shikoku, eastern Shikoku, Kii Peninsula, and, Tokai) and shallow VLFE activity into four regions (i.e. Hyuga-nada, off Cape Muroto, off the southern Kii Peninsula, and off the southeastern Kii Peninsula) according to their spatiotemporal characteristics (Figure S3).

The number of deep VLFEs detected in western Shikoku, eastern Shikoku, the Kii Peninsula, and Tokai is 895, 243, 594, and 193, respectively (Figure S4a), whereas the number of shallow VLFEs detected in Hyuga-nada, off Cape Muroto, off the southern Kii Peninsula, and off the southeastern Kii Peninsula regions is 15,249, 1,123, 168, and 1,758, respectively (Figure S4b). To discuss the relationship between the VLFE activity and interplate coupling, we estimated the cumulative moment of VLFEs for each grid. The temporal change of cumulative moment calculated by the sum of seismic moments of each VLFE, which was estimated using the amplitude magnitudes (details were described in method), yields results similar to the temporal change of total number of VLFEs (Figures 2a, 2c, and 2d). The cumulative moment of

VLFEs along the Japan and Kuril trenches detected in our previous study (Baba et al., 2020) was also estimated (Figure 2b). The classification of regions along the Japan and Kuril trenches is the same as that reported in our previous study (Baba et al., 2020).

The cumulative number and moment of deep VLFEs exhibit stepwise changes in an interval of several months accompanied by ETSs, and the rapid increase in the cumulative moment of deep VLFEs in western Shikoku in 2010 and 2019 can be modulated by long-term SSEs in the Bungo channel (Baba et al., 2018; Hirose & Obara, 2005). The spatial variation of the VLFE activity rate was evaluated using the cumulative moment density release rate, which is obtained by dividing the cumulative moment of the detected VLFEs in each grid by the analysis period and grid area. The rapid increases in the cumulative moment of shallow VLFEs off Cape Muroto can be modulated by shallow SSEs off the Kii channel (Yokota & Ishikawa, 2020) in 2009 (Mw 6.2) and 2018 (Mw 6.6; Figure 2a and 2d). The intervals of VLFE activations are longer for shallow VLFEs than for deep VLFEs and, unlike deep VLFE activity, shallow VLFE activity has no regular periodicity (Figure 2d).

The moment density release rate of deep VLFEs and its spatial variation are smaller than those of shallow VLFEs (Figure 2a). The along-strike spatial pattern of deep VLFEs is generally consistent with the distribution of energy released by deep tremors (Annoura et al., 2016). On the other hand, shallow VLFE activity shows a strong spatial heterogeneity along the Nankai Trough (Figure 2a). The largest moment density release rate was observed in the Hyuga-nada region in which earthquakes with Mw > 8 have not been recorded.

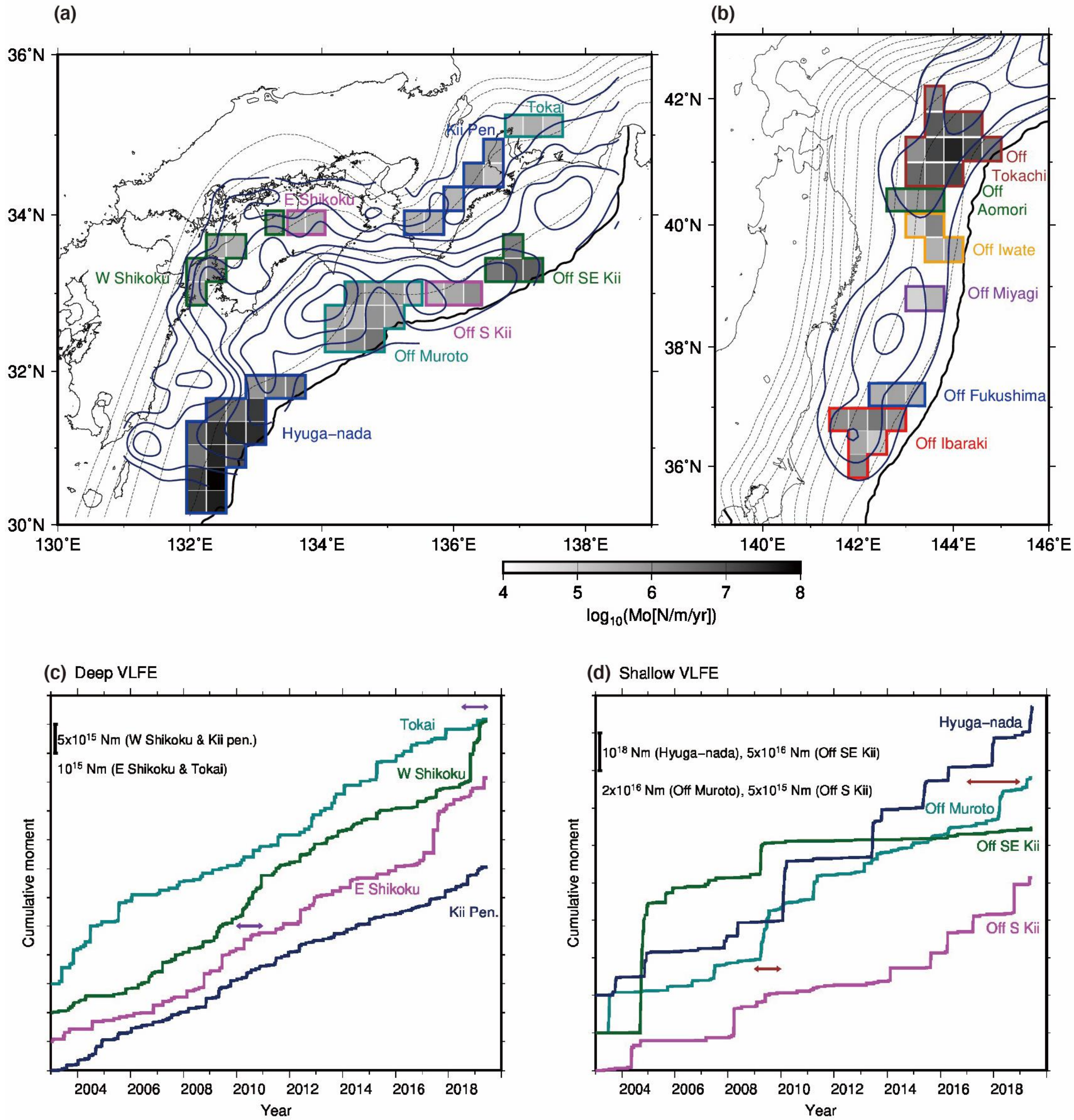

Figure 2. Moment density release rate and cumulative moments of VLFEs. (a) Distribution of the moment density release rate based on the VLFEs along the Nankai Trough. Dark blue contours show the slip-deficit rate distribution with a 10 mm/year interval (March 2005–February 2011; Noda et al., 2018). (b) Distribution of the moment density release rate based on VLFEs along the Japan and Kuril trenches. The names of the regions are based on our previous study (Baba et al., 2020). Dark blue contours indicate the slip-deficit rate distribution with a 30 mm/year interval (1996–2000; Hashimoto et al., 2012) before the 2003 Tokachi-Oki and the 2011 Tohoku earthquakes. The dashed contours and solid black curves in a and b are the same as those in Figure 1. (c) Cumulative moments of deep VLFEs. The cumulative moment of each grid was calculated by the sum of the moments of each VLFE estimated from the amplitude

magnitudes. Horizontal purple arrows indicate the periods of long-term SSEs (Ozawa, 2017) in the Bungo channel. (d) Cumulative moments of shallow VLFEs. The cumulative moment of each grid was calculated by the sum of the moments of each VLFE estimated from the amplitude magnitudes. Horizontal brown arrows indicate the periods with shallow SSEs (Yokota & Ishikawa, 2020) off the Kii channel.

4 Discussion and Conclusions

4.1. Correlation between the VLFE activity and interplate coupling

The temporal changes in the shallow VLFE activity are synchronous with the interplate coupling change after huge earthquakes. To compare the VLFE activity with the interplate coupling in both subduction zones, we determined the coupling rate by dividing the slip-deficit rate of each grid by the maximum slip-deficit rate in each subduction zone, assuming that the interplate coupling is 100% at the location of the maximum slip deficit (Hashimoto et al., 2012; Noda et al., 2018). Along the Japan Trench, the moment density release rate based on VLFEs has increased off Ibaraki and off Iwate regions and has decreased off Fukushima and off Miyagi regions since the 2011 Tohoku earthquake (Figure S5a). In addition, a Mw 8 earthquake occurred in the off Tokachi region along the Kuril Trench in the beginning of the analysis period and it has not been confirmed whether the interplate locking has been fully recovered or not (Itoh et al., 2019; Nomura et al., 2017). The moment density release rate off Tokachi continued to decrease until 2013 (Figure S5b). This tendency may indicate the recovery of the interplate locking around the coseismic slip region (Itoh et al., 2019; Nomura et al., 2017).

The strong spatial heterogeneity of shallow VLFE activity correlates well with the spatial distribution of interseismic sip deficit rate (Hashimoto et al., 2012; Noda et al., 2018) along the plate boundary (Figure 2a and 2b). The regions with a high slip-deficit rate and those with VLFE activity are separated, and VLFE activity is typically concentrated in regions surrounding areas with a high slip-deficit rate in both subduction zones. To compare the VLFE activity in preparation for the next huge earthquake, we use VLFEs along the Nankai Trough and VLFEs off Tohoku only before the 2011 Tohoku earthquake. The relationship between moment density release rate after huge earthquakes and interplate coupling rate is shown in Figure S6. The moment density release rate of shallow VLFEs and coupling rate are negatively correlated (Figure 3a). The cross-correlation coefficient between the common logarithm of the moment density release rate and coupling rate is -0.44 ± 0.14. Within huge earthquake (strong interplate coupling) areas, such as Nankai (off Muroto, off the southern Kii Peninsula, and off the southeastern Kii Peninsula) and off Tohoku (off Iwate, off Miyagi, off Fukushima, and off Ibaraki), the moment density release rate of shallow VLFEs is low (Figure 3a). In contrast, the coupling rate in Hyuga-nada is low compared with that of other shallow VLFE regions and the moment density release rate is the largest. In some regions off Tohoku, the interplate coupling is strong but the moment density release rate is relatively high. In 2008, Mw 6–7 interplate earthquakes (Nomura et al., 2019) occurred off Fukushima and off Ibaraki regions, which might have activated VLFEs. Because of this triggering process, the negative correlation between the interplate coupling rate and VLFE activity may be unclear off Tohoku regions.

In Ecuador, huge earthquakes occur in strong coupled areas, whereas SSEs release accumulated stress in weakly coupled areas in which no huge earthquakes have been recorded (Vaca et al., 2018). This tendency is the same as that in Japan: accumulated stress can be partially released by VLFEs in weakly coupled areas, whereas stress is released by large regular earthquakes in strong coupled areas. In other words, slow earthquake activity is probably related to the coupling rate.

On the other hand, deep VLFEs occur only in areas with weak interplate coupling, and the moment density release rate and its variation are small (Figure 2a). Thus, there are no meaningful spatial relationships between the moment density release rate of deep VLFEs and coupling rate (Figure 3b). In areas in which deep VLFEs occur, the proportion of the release of the accumulated stress by deep VLFEs may not be as large as that of shallow VLFEs. The annual slip rate of short-term SSEs associated with ETS in Southwest Japan was previously estimated to be 2–4 cm/year (Hirose & Obara, 2006) by previous studies is approximately half of the convergence rate of the Philippine Sea Plate. The Geodetically estimated weak coupling and small moment density release rate of VLFEs might be affected by such decoupling properties at the plate boundaries in deep slow earthquake source regions next to a stable sliding zone.

4.2. VLFE activity and seismic velocity structure

Based on the comparison between shallow VLFE activity and seismic wave velocity variation along the Nankai Trough (Wang & Zhao, 2006; Yamamoto et al., 2017), shallow VLFEs are mainly distributed within low-velocity anomalies of the bottom of the overriding plate. This tendency is similar to that reported in previous studies (Kitajima & Saffer, 2012; Takemura et al., 2019a; Tonegawa et al., 2017). As for the Japan Trench, there is a high P wave velocity (Vp) area at the bottom of the hanging wall (Zhao et al., 2011). This high Vp area corresponds to the coseismic slip area of the 2011 Tohoku earthquake; low Vp areas can be observed north and south of the high Vp area (Zhao et al., 2011). These areas correspond to areas with VLFE activity (Baba et al., 2020), such as off Iwate, off Fukushima, and off Ibaraki regions. Within the largest coseismic slip area and at the plate boundary deeper than 35 km, Vp is high and there are few VLFEs, which was also indicated by the tremor activity (Nishikawa et al., 2019).

The existence of low-velocity areas suggests a high pore fluid pressure due to rich fluid dehydrated from subducting slab (Kamei et al., 2012; Tonegawa et al., 2017). The decrease in the effective normal stress due to the high pore pressure reduces the frictional strength at the plate boundary, which triggers the generation of VLFEs with a low stress drop (Ito & Obara, 2006; Saffer & Wallace, 2015). Undrained conditions could be developed within such regions, similar to the fault planes of deep slow earthquakes (Nakajima & Hasegawa, 2016). The VLFEs may be considered to be indicators of interplate slip delineating the firmly locked portion. Off Aomori and off Tokachi regions, VLFEs actively occur but the Vp is high. This region is between the Japan and Kuril trenches regular earthquakes are rare. In addition, the afterslip of the 2003 Tokachi-Oki earthquake can continue in this region, indicating that there might be another factor activating VLFEs.

4.3. Mechanical properties of regions with VLFE activity

The VLFEs occur adjacent to large coseismic slip areas of huge earthquakes in both subduction zones of Japan. In the shallow portion, the moment density release rate of VLFEs and geodetically estimated coupling rate at the plate boundary are negatively correlated (Figure 3a). In strongly coupled areas, which correspond to the largest coseismic slip areas of huge earthquakes, the interplate frictional strength is high, which can explain the occurrence of high-speed ruptures. Because the effective strength of the plate boundary may be high in such rupture areas, the slow earthquake activity rate is low. On the other hand, in weakly coupled areas, the accumulated stress is frequently released by slow earthquakes and huge earthquake nucleation cannot be favorably initiated.

Although there are a few exceptions, the shallow VLFE activity tends to be high in areas with relatively weak interplate coupling and low seismic velocity. In areas with weak frictional conditions, shallow VLFEs can be activated by the decrease in the effective normal stress due to the high pore fluid pressure. On the other hand, the variation in the moment density release rate of deep VLFEs is smaller than that of shallow VLFEs. This suggests that the horizontal heterogeneity of the frictional properties is stronger in the shallow part of the plate boundary near the seismogenic zone than in the deep part of the plate boundary.

The results of previous studies (Saffer & Wallace, 2015; Takemura et al., 2019a; 2019b) strongly suggested that the presence of pore fluid can control the slow earthquake activity. In our previous study (Baba et al., 2020), we clarified the difference in the VLFE activity inside and outside the largest coseismic slip area of the 2011 Tohoku earthquake. In this study, we suggest that the VLFE activity is strongly related to the distribution of both the interplate coupling and pore fluid, which reflect the frictional properties at the plate boundary. The temporal changes in the VLFE activity are synchronous with the interplate coupling change due to huge earthquakes. Therefore, VLFE activity can reflect the spatiotemporal variation of interplate coupling in subduction zones.

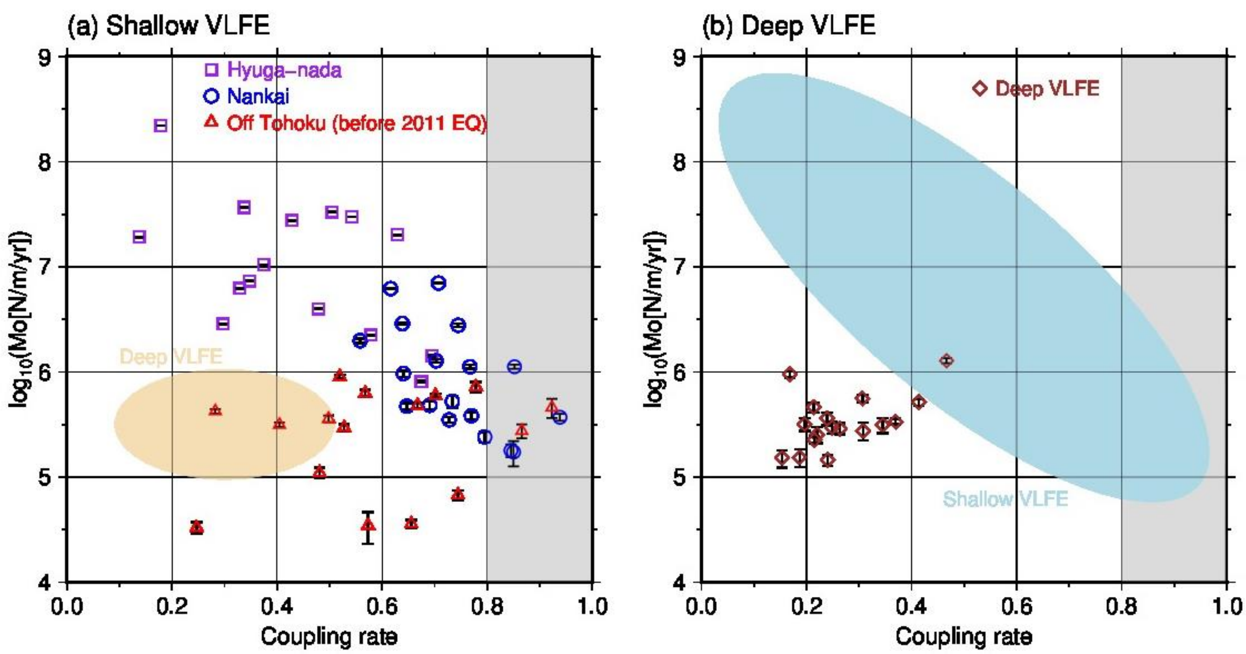

Figure 3. Relationship between the moment density release rate and interplate coupling rate. (a) Relationship between the logarithm of the cumulative moment of shallow VLFEs per year and per m^2 and coupling rate. Grey filling represents the large coupling rate area. The beige ellipse indicates the distribution of deep VLFEs. Errors of the cumulative moment in each grid were estimated by the nonparametric bootstrap method described in the Methods section. (b) Same as (a) but for deep VLFEs. The light blue ellipse indicates the distribution of shallow VLFEs.

Acknowledgments

We thank Chihiro Hashimoto and Takeshi Iinuma for providing the slip-deficit rate distribution and coseismic slip distribution of the Tohoku earthquake, respectively. The coseismic slip data of the 1944 Tonankai earthquake, 1946 Nankai earthquake, and 2003 Tokachi-Oki earthquake were derived from the Finite-Source Rupture Model Database (Mai & Thingbaijam, 2014; http://equake-rc.info/SRCMOD/). Catalogues of slow earthquakes along the Nankai trough and the Japan Trench were downloaded from the Slow Earthquake Database (Kano et al., 2018; http://www-solid.eps.s.u-tokyo.ac.jp/~sloweq/). We used F-net broadband seismograms (http://www.fnet.bosai.go.jp), National Research Institute for Earth and Disaster Resilience (2019). We used the earthquake catalogues of Japan Meteorological Agency (https://www.data.jma.go.jp/svd/eqev/data/bulletin/index_e.html) and United States Geological Survey (https://earthquake.usgs.gov/earthquakes/search/). We used OpenSWPC code Version 5.0.2 (Maeda et al., 2017; doi: 10.5281/zenodo.3712650) for numerical simulations, which were performed on the EIC computer system of the Earthquake Research Institute, the University of Tokyo. We used generic mapping tools to prepare the figures (Wessel et al., 2013). This research was supported by JSPS KAKENHI Grant in Science Research on Innovative Areas “Science of Slow Earthquakes” (JP16H06472) and JSPS Research Fellowship DC1 (JP19J20760). The VLFE catalog constructed by this study is provided in an open access repository, Zenodo (doi: 10.5281/zenodo.3724012).

References

Annoura, S., K. Obara, and T. Maeda (2016), Total energy of deep low-frequency tremor in the Nankai subduction zone, southwest Japan, *Geophysical Research Letters*, 43, 2562–2567, doi:10.1002/2016GL067780.

Araki, E., Saffer, D. M., Kopf, A. J., Wallace, L. M., Kimura, T., Machida, M., Ide, S., Davis, E., IODP Expedition 365 shipboard scientists. (2017). Recurring and triggered slow-slip events near the trench at the Nankai Trough subduction megathrust. *Science*, *356*(6343), 1157-1160. https://doi.org/10.1126/science.aan3120

Asano, Y., Obara, K., & Ito, Y. (2008). Spatiotemporal distribution of very-low frequency earthquakes in Tokachi-oki near the junction of the Kuril and Japan trenches revealed by using array signal processing. *Earth, Planets and Space*, *60*(8), 871-875. https://doi.org/10.1186/BF03352839

Baba, S., Takeo, A., Obara, K., Kato, A., Maeda, T., & Matsuzawa, T. (2018). Temporal activity modulation of deep very low frequency earthquakes in Shikoku, southwest Japan. *Geophysical Research Letters*, *45*, 733–738. https://doi.org/10.1002/2017GL076122

Baba, S., Takeo, A., Obara, K., Matsuzawa, T., & Maeda, T. (2020). Comprehensive detection of very low frequency earthquakes off the Hokkaido and Tohoku Pacific coasts, northeastern Japan. Journal of Geophysical Research, https://doi.org/10.1029/2019JB017988

DeMets, C., Gordon, R. G., Argus, D. F. & Stein, S. (1994). Effect of recent revisions to the geomagnetic reversal time scale on estimates of current plate motions. *Geophysical Research Letters*, *21*, 2191-2194. https://doi.org/10.1029/94GL02118

Hanks, T. C., & Kanamori, H. (1979). Moment magnitude scale. *Journal of Geophysical Research*, 84, 2348–2350. https://doi.org/10.1029/JB084iB05p02348

Hashimoto, C., Noda, A., & Matsu'ura M. (2012). The Mw 9.0 northeast Japan earthquake: total rupture of a basement asperity. *Geophysical Journal International*, 189, 1-5. https://doi.org/10.1111/j.1365-246X.2011.05368.x

Hirose, H., Asano, Y., Obara, K., Kimura, T., Matsuzawa, T., Tanaka, S., & Maeda, T. (2010). Slow earthquakes linked along dip in the Nankai subduction zone. *Science*, *330*(6010), 1502. https://doi.org/10.1126/Science.1197102

Hirose, H., & Obara, K. (2005). Repeating short- and long-term slow slip events with deep tremor activity around the Bungo channel region, southwest Japan. *Earth, Planets and Space*, *57*(10), 961–972. https://doi.org/10.1186/BF03351875

Hirose, H. & Obara, K. (2006). Short-term slow slip and correlated tremor episodes in the Tokai region, central Japan. *Geophysical Research Letters*, 33, L17311. https://doi.org/10.1029/2006GL026579

Iinuma, T., Hino, R., Kido, M., Inazu, D., Osada, Y., Ito, Y., Ohzono, M., Tsushima, H., Suzuki, S., Fujimoto, H., & Miura, S. (2012). Coseismic slip distribution of the 2011 off the Pacific of Tohoku earthquake (M9.0) refined by means of seafloor geodetic data. *Journal of Geophysical Research*, *117*, B07409. https://doi.org/10.1029/2012JB009186

Ito, Y. & Obara, K. (2006). Dynamic deformation of the accretionary prism excites very low frequency earthquakes. *Geophysical Research Letters*, *33*, L02311, https://doi.org/10.1029/2005GL025270

Ito, Y., Obara, K., Shiomi, K., Sekine, S., & Hirose, H. (2007). Slow earthquakes coincident with episodic tremors and slow slip events. *Science*, *315*(5811), 503–506. https://doi.org/10.1126/science.1134454

Itoh, Y., Nishimura, T., Ariyoshi, K., & Matsumoto, H. (2019). Interplate slip following the 2003 Tokachi - oki earthquake from ocean bottom pressure gauge and land GNSS data. *Journal of Geophysical Research*, 124, 4205–4230. https://doi.org/ 10.1029/2018JB016328

Kamei, R., Pratt, R. G., and Tsuji, T. (2012). Waveform tomography imaging of a megasplay fault system in the seismogenic Nankai subduction zone. *Earth and Planetary Science Letters*, 317-318, 343-353. https://doi.org/10.1016/j.epsl.2011.10.042

Kano, M., Aso, N., Matsuzawa, T., Ide, S., Annoura, S., Arai, R., Baba, S., Bostock, M., Chao, K., Heki, K., Itaba, S., Ito, Y., Kamaya, N., Maeda, T., Maury, J., Nakamura, M., Nishimura, T., Obana, K., Ohta, K., Poiata, N., Rousset, B., Sugioka, H., Takagi, R., Takahashi, T., Takeo, A., Tu, Y., Uchida, N., Yamashita, Y., & Obara, K. (2018). Development of a Slow Earthquake Database, *Seismological Research Letters*, *89*(4), 1566-1575, https://doi.org/10.1785/0220180021

Kikuchi, M., Nakamura, M., & Yoshikawa, K. (2003). Source rupture processes of the 1944 Tonankai earthquake and the 1945 Mikawa earthquake derived from low-gain seismograms. *Earth, Planets and Space*, 55, 159-172. https://doi.org/10.1186/BF03351745

Kitajima, H., & Saffer, D. Elevated pore pressure and anomalously low stress in regions of low frequency earthquakes along the Nankai Trough subduction megathrust. *Geophysical Research Letters*, 39, L23301. (2012). https://doi.org/10.1029/2012GL053793

Koketsu, K., Miyake, H., & Suzuki, H. (2012). Japan Integrated Velocity Structure Model Version 1. In: *Proceedings of the 15th World Conference on Earthquake Engineering*, Lisbon, Portugal, 24 - 28 September, Paper 1773.

Maeda, T., Takemura, S., & Furumura, T. (2017). OpenSWPC: An open-source integrated parallel simulation code for modeling seismic wave propagation in 3D heterogeneous viscoelastic media, *Earth, Planets and Space, 69*, 102. https://doi.org/10.1186/s40623-017-0687-2

Mai, P.M. and Thingbaijam, K.K.S. (2014). SRCMOD: An online database of finite - fault rupture models. *Seismological Research Letters*, 85(6), pp.1348-1357.

Matsuzawa, T., Asano, Y., & Obara, K. (2015). Very low frequency earthquakes off the Pacific of Tohoku, Japan. *Geophysical Research Letters*, *42*, 4318–4325. https://doi.org/10.1002/2015GL063959

Nakajima, J., & Hasegawa, A. (2016). Tremor activity inhibited by well-drained conditions above a megathrust. *Nature Communications*, 7, 13863. https://doi.org/10.1038/ncomms13863

Nakano, M., Hori, M., Araki, E., Kodaira, S., & Ide, S. (2018). Shallow very-low-frequency earthquakes accompany slow slip events in the Nankai subduction zone. *Nature Communications*, *9*, 984. https://doi.org/10.1038/s41467-018-03431-5

National Research Institute for Earth Science and Disaster Resilience (2019). NIED F-net. https://doi.org/10.17598/NIED.0005

Nishikawa, T., Matsuzawa, T., Ohta, K., Uchida, N., Nishimura, T., & Ide, S. (2019). The slow earthquake spectrum in the Japan Trench illuminated by the S - net seafloor observatories. *Science*, 365, 808–813. https://doi.org/10.1126/science.aax5618

Noda, A., Saito, T., & Fukuyama, E. (2018). Slip - deficit rate distribution along the Nankai Trough, southwest Japan, with elastic lithosphere and viscoelastic asthenosphere. *Journal of Geophysical Research*, 123, 8125–8142. https://doi.org/10.1029/2018JB015515

Nomura, S., Ogata, Y., Uchida, N., & Matsu'ura, M. (2017). Spatiotemporal variations of interplate slip rates in northeast Japan inverted from recurrence intervals of repeating earthquakes. *Geophysical Journal International*, 208(1), 468–481. https://doi.org/10.1093/gji/ggw395

Obara, K. (2002). Nonvolcanic deep tremor associated with subduction in southwest Japan. *Science*, *296*(5573), 1679–1681. https://doi.org/10.1126/science.1070378

Obara, K., & Ito, Y. (2005). Very low frequency earthquakes excited by the 2004 off the Kii peninsula earthquakes: A dynamic deformation process in the large accretionary prism. *Earth, Planets and Space*, *57*(4), 321-326. https://doi.org/10.1186/BF03352570

Obara, K. & Kato, A. (2016). Connecting slow earthquakes to huge earthquakes. *Science*, 353, 253–257. https://doi.org/10.1126/science.aaf1512

Obara, K., Tanaka, S., Maeda, T., & Matsuzawa, T. (2010). Depth-dependent activity of non-volcanic tremor in southwest Japan. *Geophysical Research Letters*, *37*(13), L13306. https://doi.org/10.1029/2010GL043679

Okada, Y., Kasahara, K., Hori, S., Obara, K., Sekiguchi, S., Fujiwara, H., & Yamamoto, A. (2004). Recent progress of seismic observation networks in Japan – Hi-net, F0net, K-net and KiK-net. *Earth, Planets and Space*, *56*(8), 15-18. https://doi.org/10.1186/BF03353076

Ozawa, S. (2017). Long-term slow slip events along the Nankai trough subduction zone after the 2011 Tohoku earthquake in Japan. *Earth, Planets and Space*, *69*(19), 56. https://doi.org/10.1186/s40623-017-0640-4

Rogers, G., & Dragert, H. (2003). Episodic tremor and slip on the Cascadia subduction zone: The chatter of silent slip. *Science*, *300*(5627), 1942–1943. https://doi.org/10.1126/science.1084783

Saffer, D. M., & Wallace, L. M. (2015). The frictional, hydrologic, metamorphic and thermal habitat of shallow slow earthquakes. *Nature Geoscience*, 8(8), 594–600. https://doi.org/10.1038/ngeo2490

Sugioka, H., Okamoto, T., Nakamura, T., Ishihara, Y., Ito, A., Obana, K., et al. (2012). Tsunamigenic potential of the shallow subduction plate boundary inferred from slow seismic slip. *Nature Geoscience*, 5(6), 414–418. https://doi.org/10.1038/ngeo1466

Syracuse, E., M., van Keken, P., E., & Abers, G. A. (2010). The global range of subduction zone thermal models. *Physics of the Earth and Planetary Interiors*, 183, 73-90. https://doi.org/10.1016/j.pepi.2010.02.004

Takemura, S., Matsuzawa, T., Noda, A., Tonegawa, T., Asano, Y., Kimura, T., & Shiomi, K. (2019a). Structural characteristics of the Nankai Trough shallow plate boundary inferred from shallow very low frequency earthquakes. *Geophysical Research Letters*, 46, 4192-4201. https://doi.org/10.1029/2019GL082448

Takemura, S., Noda, A., Kubota, T., Asano, Y., Matsuzawa, T., & Shiomi, K. (2019b). Migrations and Clusters of Shallow Very Low Frequency Earthquakes in the Regions Surrounding Shear Stress Accumulation Peaks Along the Nankai Trough. *Geophysical Research Letters*, 46(21), 11830-11840. https://doi.org/10.1029/ 2019GL084666

Tanaka, S., Matsuzawa, T., & Asano, Y. (2019). Shallow low - frequency tremor in the northern Japan Trench subduction zone. *Geophysical Research Letters*, *46*, 5217-5224. https://doi.org/10.1029/2019GL082817

Tanioka, Y., & Satake, K. (2001). Coseismic slip distribution of the 1946 Nankai earthquake and aseismic slips caused by the earthquake. *Earth, Planets and Space*, 53, 235-241. https://doi.org/10.1186/BF03352380

Tichelaar, B. W., & Ruff L. J. (1989). How good are our best models? Jackknifing, bootstrapping, and earthquake depth, *Eos, Transactions American Geophysical Union*, 70, 593. https://doi.org/10.1029/89EO00156

Tonegawa, T., Araki, E., Kimura, T., Nakamura, T., Nakano, M., & Suzuki, K. (2017). Sporadic low - velocity volumes spatially correlate with shallow very low frequency earthquake clusters. *Nature Communications*, 8(1), 1–7. https://doi.org/10.1038/s41467-017-02276-8

Vaca, S., Vallée, M., Nocquet, J., Battaglia, J., & Régnier, M. (2018). Recurrent slow slip events as a barrier to the northward rupture propagation of the 2016 Pedernales earthquakes (Central Ecuador). *Tectonophysics*, 724-725, 80-92. https://doi.org/10.1016/j.tecto.2017.12.012

Wallace, L. M., Beaven. J., Bannister, S., & Williams, C. (2012). Simultaneous long-term and short-term slow slip events at the Hikurangi subduction margin, New Zealand: Implications for processes that control slow slip event occurrence, duration, and migration. *Journal of Geophysical Research*, 117, B11402. https://doi.org/10.1029/2012JB009489

Wang, Z., & Zhao, D. Vp and Vs tomographyof Kyushu, Japan: New insight into arc magmatism and forearc seismotectonics. *Physics of the Earth and Planetary Interiors*, 157, 269-285. (2006). https://doi.org/10.1016/j.pepi.2006.04.008

Wessel, P., Smith, W. H. F., Scharroo, R., Luis, J., & Wobbe, F. (2013). Generic Mapping Tools: Improved Version Released. *Eos, Transactions American Geophysical Union*, *94*(45), 409–410. https://doi.org/10.1002/2013EO450001

Yagi, Y. (2004). Source rupture process of the 2003 Tokachi-oki earthquake determined by joint inversion of teleseismic body wave and strong ground motion data, *Earth, Planets and Space*, *56*(3), 311–316. https://doi.org/10.1186/BF03353057

Yamamoto, Y., Takahashi, T., Kaiho, Y., Obana, K., Nakanishi, A., Kodaira, S., & Kaneda, Y. Seismic structure off the Kii Peninsula, Japan, deduced from passive and active-source seismographic data. *Earth and Planetary Science Letters*, 461, 163-175. (2017). https://doi.org/10.1016/j.epsl.2017.01.003

Yamashita Y., Yakiwara, H., Asano, Y., Shimizu, H., Uchida, K., Hirao, S., Umakoshi, K., Miyamachi, H., Nakamoto, M., Fukui, M., Kamizono, M., Kanehara, H., Yamada, T., Shinohara, M., & Obara, K. (2015). Migrating tremor off southern Kyushu as evidence for slow slip of a shallow subduction interface, *Science*, *348*(6235), 676-679. https://doi.org/10.1126/science.aaa4242

Yokota, Y., & Ishikawa, T. (2020). Shallow slow slip events along the Nankai Trough detected by the GNSS-A. *Science Advances*, 6, eaay5786. htts://doi.org/10.1126/sciadv.aay5786

Zhao, D., Huang,Z., Umino, N., Hasegawa, A., & Kanamori, H. (2011). Structural heterogeneity in the megathrust zone and mechanism of the 2011 Tohoku-oki earthquake (M2 9.0). *Geophysical Research Letters*, 38, L17308. https://doi.org/10.1029/2011GL048408

Geophysical Research Letters

Supporting Information for

Slow earthquakes illuminating interplate coupling heterogeneities in subduction zones

Satoru Baba[1], Shunsuke Takemura[1], Kazushige Obara[1], and Akemi Noda[2]

1. Earthquake Research Institute, The University of Tokyo
2. National Research Institute for Earth Science and Disaster Resilience

Contents of this file

Text S1
Figures S1 to S6

Additional Supporting Information (Files uploaded separately)

Data Set S1

Introduction

This supporting information file includes one supplemental text and six supplemental figures. Text S1 describes the error of the cumulative moment of each grid. Figure S1 presents the virtual epicentral grids analysed in this study. Figure S2 presents the frequency distribution of VLFEs. Figure S3 presents the distribution of the number of detected events in each virtual epicentral grid. Figure S4 presents the cumulative numbers of events detected from January 2003 to June 2019. Figure S5 presents the temporal variation of the moment density release rate. Figure S6 presents the relationship between the moment density release rate after huge earthquakes and interplate coupling rate.

Additional Supporting Information includes the detected VLFE catalog (Data Set S1).

Text S1.

Error estimation

We evaluated the errors of the cumulative moment of each grid by using the nonparametric bootstrap method (Tichelaar & Ruff, 1989). First, 500 bootstrap samples were prepared for each grid. A bootstrap sample was generated from the original events. If n events were detected in a grid, a bootstrap sample consisted of *n* events including duplicates. Subsequently, cumulative moments were calculated by the sum of the moments of *n* events. Finally, we estimated the standard deviations of the 500 cumulative moments.

We also estimated the errors of the cross-correlation coefficients between the moment density release rate and the coupling ratio using the nonparametric bootstrap method. The 500 bootstrap samples, which were generated from the 49 original grids, were prepared and a bootstrap sample consisted of 49 grids including duplicates. Cross-correlation coefficients were calculated for each bootstrap sample. We then estimated the standard deviations of the 500 cross-correlation coefficients.

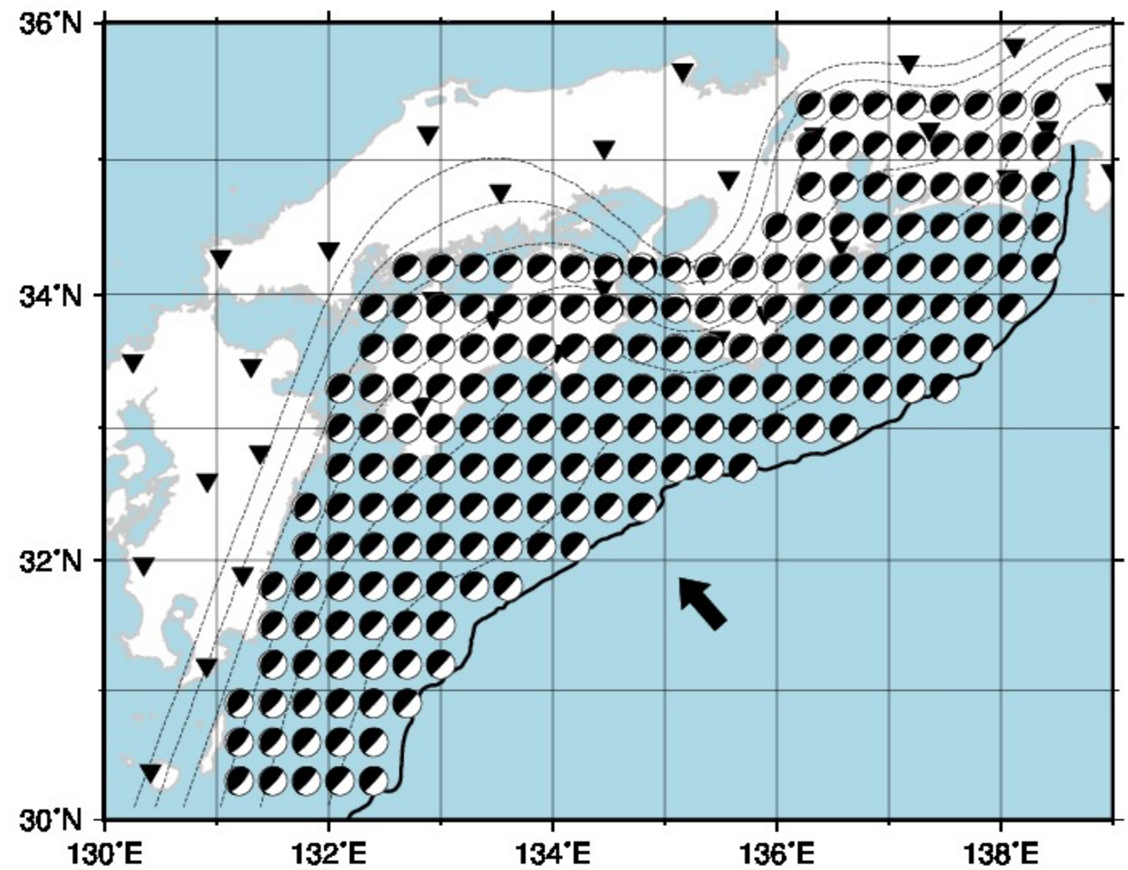

Figure S1. Virtual epicentral grids analysed in this study. Beach balls indicate the places and focal mechanisms of virtual sources. Inverted triangles represent the F-net station locations used in this study. The black line, black arrows, and dashed contours are the same as those in Figure 1.

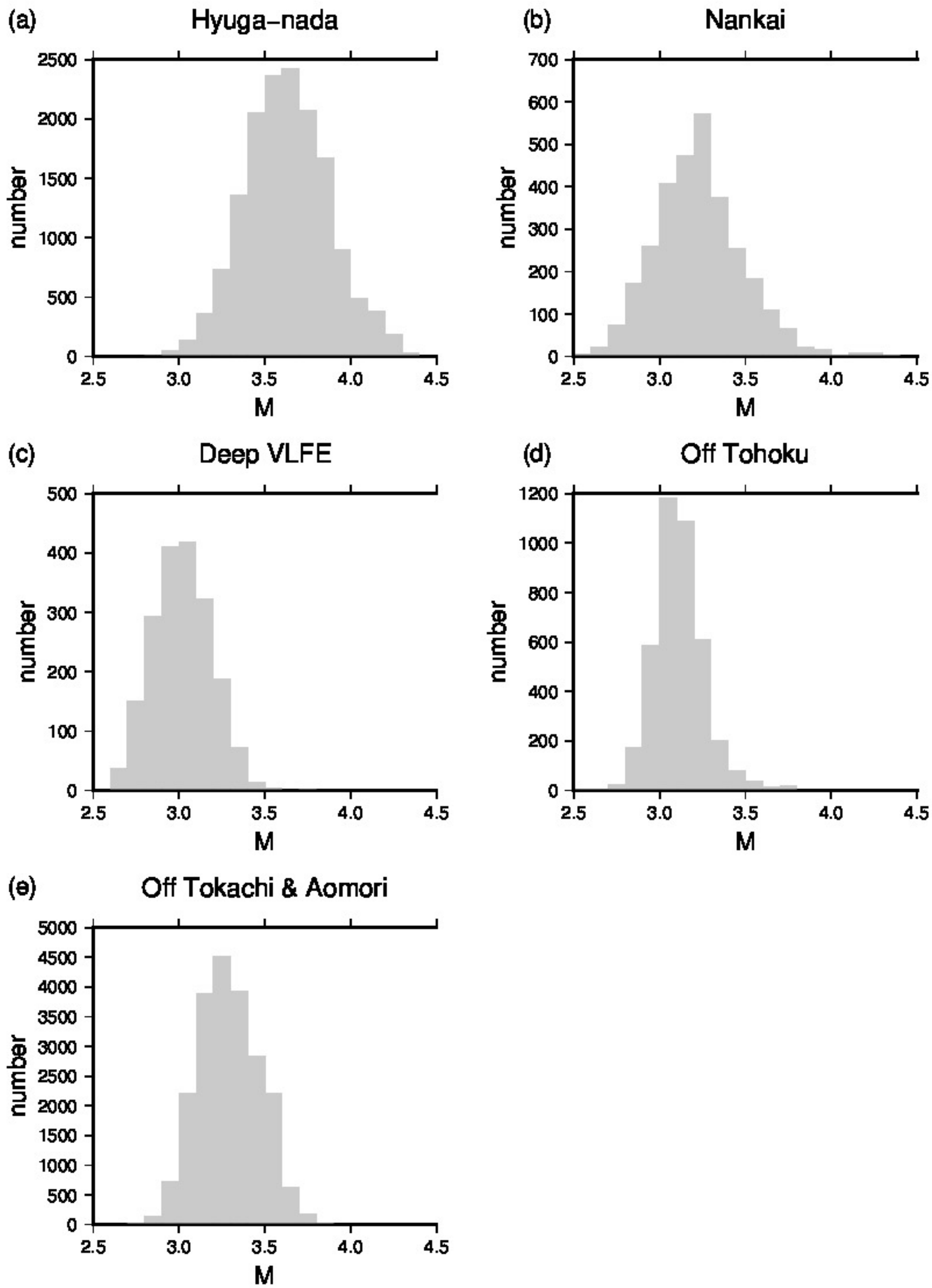

Figure S2. Frequency distribution of VLFEs. (a) Shallow VLFEs in Hyuga-nada, (b) Shallow VLFEs in Nankai, except for Hyuga-nada, (c) Deep VLFEs along the Nankai Trough, (d) Off Tohoku region, and (e) Off Tokachi and off Aomori.

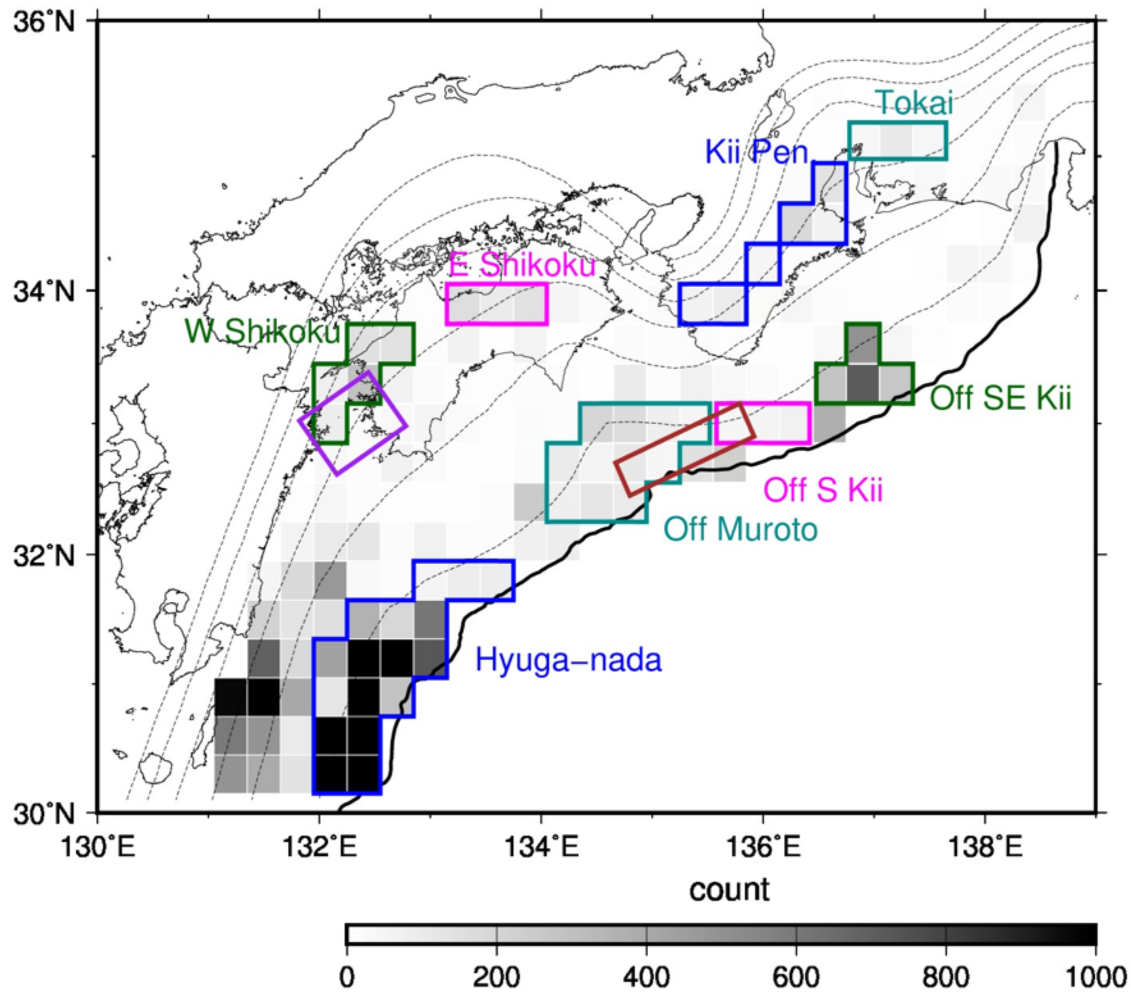

Figure S3. Distribution of the number of detected events in each virtual epicentral grid. The black line, dashed contours, and purple and brown rectangles are the same as those in Figure 1.

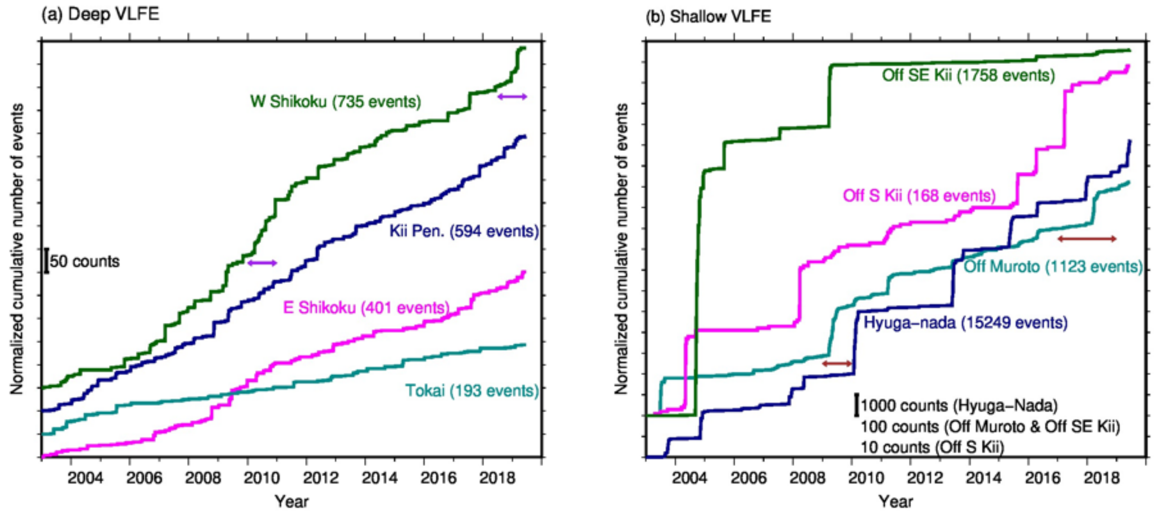

Figure S4. Cumulative numbers of events detected from January 2003 to June 2019. (a) Cumulative numbers of deep VLFEs. The cumulative number of each group contains events from all virtual epicentral grids in that group. The horizontal purple arrows are the same as those in Figure 2c. (b) Cumulative numbers of shallow VLFEs. The cumulative number of each group contains events from all virtual epicentral grids in that group. The horizontal brown arrows are the same as those in Figure 2d.

(a)

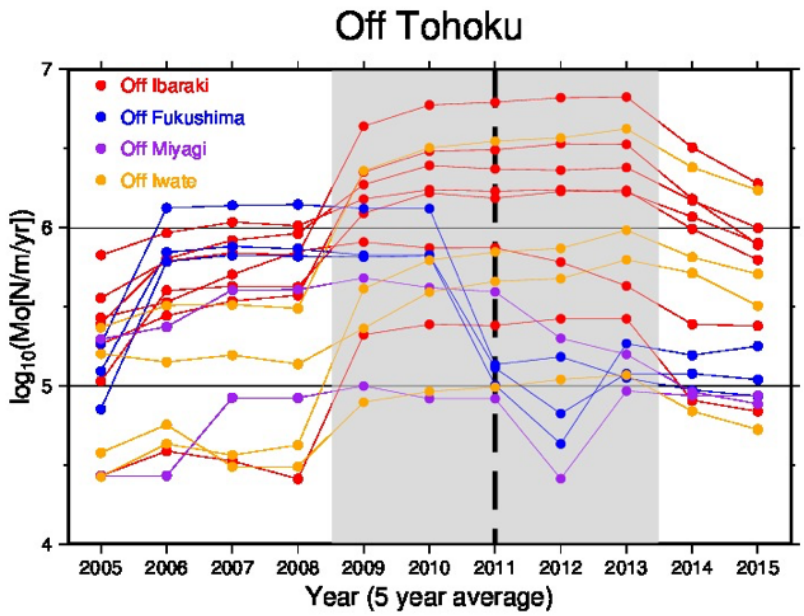

(b)

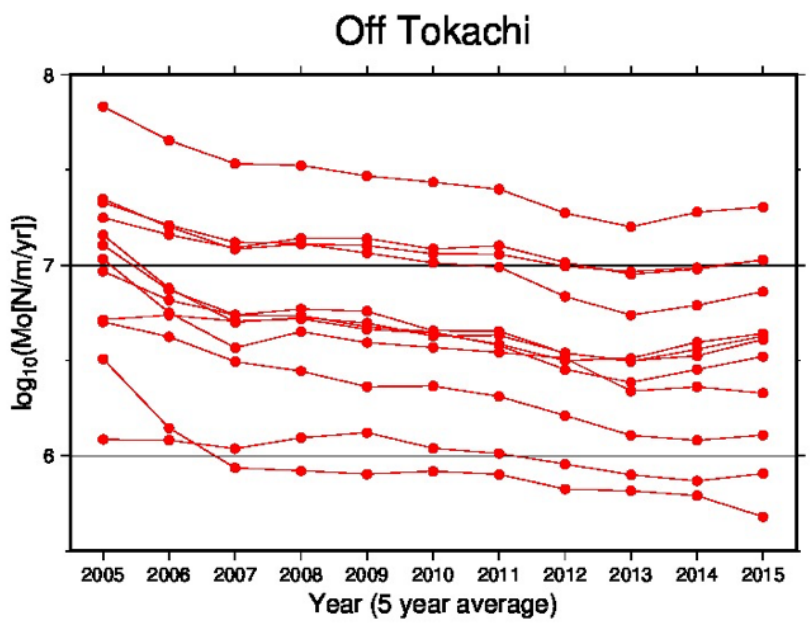

Figure S5. Temporal variation of the moment density release rate. (a) Temporal variation of the moment density release rate for each grid based on the 5-year moving average off Tohoku. The black broken line shows the year of the Tohoku earthquake. The period, which includes the year of the Tohoku earthquake based on the 5-year moving average, is filled in grey. (b) Same as (a) but for the region off Tokachi.

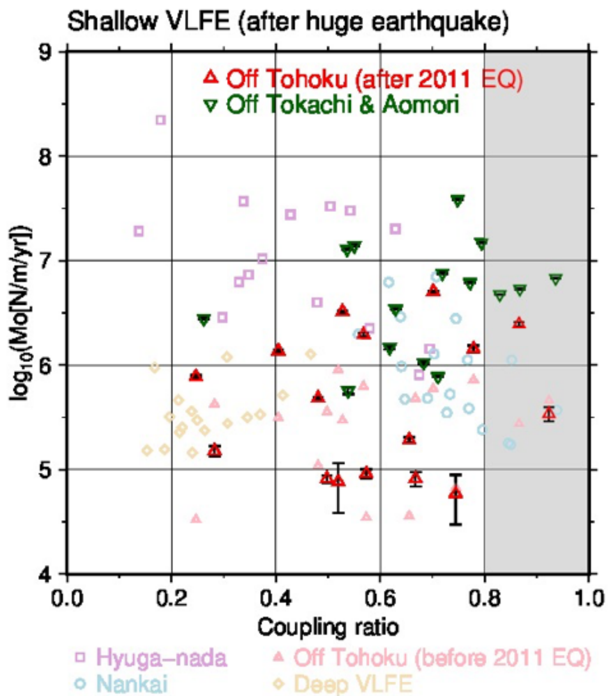

Figure S6. Relationship between the moment density release rate after huge earthquakes and interplate coupling ratio. Same as Figure 3 but for shallow VLFEs that occurred after huge earthquakes. Light symbols indicate the distribution of deep VLFEs and shallow VLFEs before huge earthquakes.

Data Set S1. List of origin times of detected VLFEs. First column: year, second column: month, third column: day, forth column: hour, fifth column: minute, sixth column: second, seventh column: longitude, eighth column: latitude, ninth column: depth, and tenth column: region name. Times are described in JST (UT+9).